Hindawi
Advances in High Energy Physics
Volume 2018, Article ID 4176840, 20 pages
https://doi.org/10.1155/2018/4176840

Research Article

Study of Rare Mesonic Decays Involving Di-Neutrinos in Their Final State

Azeem Mir,[1] Farida Tahir,[1] Shakeel Mahmood ,[2] and Shi- Hai Dong [3]

[1] *Physics Department, COMSATS Institute of Information Technology, Islamabad, Pakistan*
[2] *Air University, PAF Complex, Service Road, E-9, Islamabad, Pakistan*
[3] *CIDETEC, Instituto Politécnico Nacional, Unidad Profesional, Adolfo López Mateos, CDMX 07700, Mexico*

Correspondence should be addressed to Shakeel Mahmood; shakeel_mahmood@hotmail.com

Received 1 December 2017; Revised 15 March 2018; Accepted 11 April 2018; Published 1 August 2018

Academic Editor: Adrian Buzatu

We have studied phenomenological implication of R-parity violating ($\not{R}_p$) Minimal Supersymmetric Model (MSSM) via analyses of pure leptonic ($M \longrightarrow \nu\overline{\nu}$) and semileptonic decays of pseudoscalar mesons ($M \longrightarrow X\nu\overline{\nu}$). These analyses involve comparison between theoretical predictions made by $\not{R}_p$ MSSM and the Standard Model (SM) with the experimental results like branching fractions (Br) of the said process. We have found, in general, that $\not{R}_p$ contribution dominates over the SM contribution, i.e., by a factor of 10 for the pure leptonic decays of $K_{L,S}$ and by 10^2 and 10^4 in case of B_s and B_d, respectively. Furthermore, the limits obtained on $\not{R}_p$ Yukawa couplings ($\lambda'_{\alpha k\beta}\lambda'^{*}_{\alpha k\gamma}$) by using Br ($M \longrightarrow X\nu\overline{\nu}$) are used to calculate Br ($M \longrightarrow \nu\overline{\nu}$). This demonstrates the role of $\not{R}_p$ MSSM as a viable model for the study of new physics contribution in rare decays at places like Super B factories, KOTO (J-PARC) and NA62 at CERN.

1. Introduction

Flavor Changing Neutral Currents (FCNC) that mediate different flavored fermions (quarks) of the same charge are one of the most important tools searching for physics beyond the Standard Model (SM). This is due to their rarity owing to the GIM mechanism [1]. FCNC processes involving leptons are strictly forbidden in SM due to lepton family number conservation contrary to established experimental facts [2–13], and such processes can only be accommodated through physics beyond the SM. However, *lepton flavor* conserving processes can proceed through both universal and non-universal weak neutral current interactions. Here, universal weak neutral current interactions correspond to the SM interactions, which are flavor as well as generation blind, and non-universal weak neutral current interactions represent new physics (NP) interactions which are flavor as well as generation sensitive. Analyses, involving the bounds on NP couplings, of such type of processes are good for comparative study of different models. In this paper, we have presented one class of such type of pure leptonic and semileptonic decays of pseudoscalar mesons involving di-neutrinos in their final state in the framework of SM and R-parity violating ($\not{R}_p$) supersymmetric (SUSY) model.

Leptonic and semileptonic decays of beauty and strange mesons have played an important role in measuring parameters related to Cabibbo-Kobayashi-Maskawa (CKM), unitary angles, and also in probing CP-violation [14–16]. Many NP models like 2HDM [17] and $\not{R}_p$ Minimal Supersymmetric Standard Model (MSSM) [18–20] have been explored in these processes [21–33] as well. Super B factories [34, 35] and experimental set-ups like KOTO at J-PARC and NA62 at CERN [36–39] hold a lot of potential in this regard. LHCb also holds a lot of promise for discovering prospects of NP in B decays [40, 41].

MSSM [42–47] is the most economical version of SUSY. It is also the minimal extension of SM [42–47]. MSSM allows processes that violate baryon and lepton number. It also allows Lepton flavor violating (LFV) processes (that do violate lepton family number). R-parity, a discrete symmetry, is imposed to prevent baryon number, lepton number, and flavor violating processes. It is defined as $R_p = (-1)^{3B+L+2S}$ [42, 48, 49]. R-parity conservation is phenomenologically motivated and if relaxed carefully allows one to analyze rare and forbidden decays while maintaining the stability of matter [46, 50–52]. The R-parity violating gauge invariant and renormalizable superpotential is [42, 48, 49]

$$W_{\not{R}_p} = \frac{1}{2}\lambda_{ijk}L_iL_jE_k^c + \lambda'_{ijk}L_iQ_jD_k^c + \frac{1}{2}\lambda''_{ijk}U_i^C D_j^C D_k^C + \mu_i H_u L_i, \quad (1)$$

where i, j, k are generation indices, L_i and Q_i are the lepton and quark left-handed $SU(2)_L$ doublets, and E^c, D^c are the charge conjugates of the right-handed leptons and quark singlets, respectively. Here λ_{ijk}, λ'_{ijk}, and λ''_{ijk} are the Yukawa couplings. The term proportional to λ_{ijk} is antisymmetric in first two indices $[i, j]$ and λ''_{ijk} is antisymmetric in last two indices $[j, k]$, implying $9(\lambda_{ijk}) + 27(\lambda'_{ijk}) + 9(\lambda''_{ijk}) = 45$ independent coupling constants among which 36 are related to the lepton flavor violation (9 from LLE^c and 27 from LQD^c). We can rotate the last term away without affecting things of our interest.

In this scenario for detailed illustration we will use the pure and semileptonic rare decays of pseudoscalar mesons with neutrinos in the final state, i.e., $M^0 \longrightarrow \nu_\alpha\overline{\nu}_\beta, M^{\pm,0} \longrightarrow N^{\pm,0}\nu_\alpha\overline{\nu}_\beta$, and $M^{\pm,0} \longrightarrow N^{\pm,0}\nu_\alpha\overline{\nu}_\beta$, where $M = K, B$ and $N = \pi, K$. At the quark level, all $M^{\pm,0} \longrightarrow N^{\pm,0}\nu_\alpha\overline{\nu}_\beta$ decays are represented by $s(b) \longrightarrow d(d,s)q\nu_\alpha\overline{\nu}_\beta$ $(q = d, s)$ and (all these processes can be) divided into two categories on the bases of lepton flavors, i.e.,

(1) *lepton flavor conserving* $(\alpha = \beta)$,

(2) *lepton flavor violating* $(\alpha \neq \beta)$ decays.

The *first type* of decays $s(b) \longrightarrow d(d,s)\nu_\alpha\overline{\nu}_\alpha$ $(\alpha = e, \mu, \tau)$ is absent in the SM at tree level and is however induced by GIM mechanism [1] at the quantum loop level [53] which makes their effective strength very small, further suppression caused by the CKM matrix [54, 55]. These two suppressions make FCNC decays very rare. Furthermore, these processes will provide indirect test of high energy scales through a low energy process. Such type of processes has only short distance dominant contribution whereas long distance contribution is subleading [56], as we are taking pure and semileptonic decays, which can be accurately predicted in the SM due to the fact that the only relevant hadronic operators are just the current operators whose matrix elements can be extracted from their respective leading decays [57–61].

The *second type* of decays $s(b) \longrightarrow d(d,s)\nu_\alpha\overline{\nu}_\beta$ $(\alpha \neq \beta;\ \alpha, \beta = e, \mu, \tau)$ is strictly forbidden to all orders in the SM due to lepton flavor violation, so their detection can clearly signal the presence of new interactions. Hence one can say that these are the "golden channels" for the study of NP.

In this paper, we have analyzed the above-mentioned decays in the SM (first case) and then in $\not{R}_p$ violating MSSM. Our focus is to compare the NP contribution to the branching fraction of decay processes (under consideration) with the SM prediction and also with the experimental limits. In the forthcoming section, we will discuss these processes one by one.

2. $s \longrightarrow d\nu_\alpha\overline{\nu}_\alpha$

In the SM, the effective Hamiltonian for the semileptonic $(K \longrightarrow \pi\nu_\alpha\overline{\nu}_\alpha, K \longrightarrow \pi^0\nu_\alpha\overline{\nu}_\alpha)$ and pure leptonic $K_{L,S} \longrightarrow \nu_\alpha\overline{\nu}_\alpha$ processes is given by [62, 63]

$$H_{eff} = \sum_l C_{SM}\,(\overline{s}d)_{V-A}\,(\overline{\nu}_l\nu_l)_{V-A}. \quad (2)$$

In this case, all leptons couple universally with the electroweak gauge bosons, where

$$C_{SM} = \frac{G_F\alpha}{2\sqrt{2}\sin^2\theta_w}\left(V_{cs}^*V_{cd}X_{NL}^l + V_{ts}^*V_{td}X(x_t)\right),$$
$$X(x_t) = X_0(x_t) + \frac{\alpha_S}{4\pi}X_l(x_t), \quad (3)$$

where $X_0(x_t) = (x_t/8)((x_t+2)/(x_t-1) + ((3x_t-6)/(x_t-1)^2)\log x_t)$ and

$$X_l(x_t) = \frac{-23x_t + 5x_t^2 - 4x_t^3}{3(1-x_t)^2} + \frac{x_t - 11x_t^2 + x_t^3 + x_t^4}{(1-x_t)^3}\log x_t + \frac{8x_t + 4x_t^2 + x_t^3 - x_t^4}{2(1-x_t)^3}(\log x_t)^2 - \frac{4x_t - x_t^3}{(1-x_t)^2}\int_1^{x_t} dt\frac{\log t}{1-t} + \gamma_m^{(0)}x_t\frac{\partial X_0(x_t)}{\partial x_t}\log\frac{\mu_t^2}{M_W^2}, \quad (4)$$
$$X_{NL}^l = C_{NL} - 4B_{NL}^{(1/2)},$$

and $x_t = \overline{m}_t^2(\mu_t)/M_W^2$, $\mu_t = O(m_t), C_{NL}$ and $B_{NL}^{(1/2)}$ are Z^0 penguin and box diagrams, respectively. $V_{cs}^*V_{cd}$ are CKM matrix elements and α_S is the coupling strength of strong interactions.

In MSSM, the relevant effective Lagrangian for the decay process $K \longrightarrow \pi\nu_\alpha\overline{\nu}_\alpha$ is given by [57–61]

$$L_{\not{R}_p}^{eff}(s \longrightarrow d + \nu_\alpha + \overline{\nu}_\alpha) = \frac{4G_F}{\sqrt{2}}\left[A_{\alpha\beta}^{sd}\left(\overline{\nu}_\alpha\gamma^\mu P_L\nu_\alpha\right)\left(\overline{d}\gamma_\mu P_R s\right)\right], \quad (5)$$

where $\alpha = e, \mu$. The first term in (2) comes from the down squark exchange (where d and s are down type quarks). The dimensionless coupling constant $A_{\alpha\alpha}^{sd}$ is related to $\not{R}_p$ Yukawa couplings $\lambda'_{\alpha k1}\lambda'^*_{\alpha k2}$ by

$$A_{\alpha\alpha}^{sd} = \frac{\sqrt{2}}{4G_F}\sum_{k=1}^{3}\frac{\lambda'_{\alpha k1}\lambda'^*_{\alpha k2}}{2m_{\tilde{d}_k^c}^2}. \quad (6)$$

The differential decay rate $d\Gamma/dq^2$ for the semileptonic decay processes is given by [62–64]

$$\frac{d\Gamma}{dq^2} = \frac{1}{2^5\pi^5}\lambda^{3/2}\left(1, r_M, s\right) m_K^3 \left|f_p^+\left(q^2\right)\right|^2 \left|C_l\right|^2, \quad (7)$$

where $\lambda(1, r_M, s) = 1 + r_M^2 + s^2 - 2r_M - 2s - 2r_M s$ with $r_M = (m_M/m_B)^2$ and $s = q^2/m_B^2$, $C_l = C_{SM} + z(1/8)e^{i\theta}$; z is the general NP parameter. We have used the value for the form factor $f_p^+(q^2)$ for the above decay processes of K^+ and K^0 as given in [65]. Since this work focuses on $\not{R}_p$ MSSM, we will shift our focus to z (for the calculation of limits on couplings) and Yukawa couplings $\lambda'_{\alpha k1}\lambda'^*_{\alpha k2}/m^2_{\tilde{d}^c_k}$ (for the predictions of branching fraction). The decay rate for pure leptonic decay processes is given by

$$\Gamma\left(s \longrightarrow d\nu_l\overline{\nu}_l\right) = \frac{1}{8\pi}m_K^3\left|f_p\left(q^2\right)\right|^2\left|\frac{2m_l}{m_K}C_l\right|^2. \quad (8)$$

The form factor $f_p(q^2)$ is given by [66]. m_K represents the mass of strange meson and m_l is the mass of lepton, where C_l is same as that of semileptonic decays.

3. $b \longrightarrow d(s)\nu_\alpha\nu_\alpha$

In MSSM, the relevant effective Lagrangian for the decay process $B \longrightarrow \pi(K)\nu_\alpha\overline{\nu}_\alpha$ is given by [57–61]

$$\begin{aligned} L^{eff}_{\not{R}_p}&\left(b \longrightarrow d\left(s\right) + \nu_\alpha + \overline{\nu}_\alpha\right) \\ &= \frac{4G_F}{\sqrt{2}}\left[A^{bd(s)}_{\alpha\alpha}\left(\overline{\nu}_\alpha\gamma^\mu P_L\nu_\alpha\right)\left(\overline{b}\gamma_\mu P_R d\left(s\right)\right)\right], \end{aligned} \quad (9)$$

where $\alpha = e, \mu$. The first term in (2) comes from the down squark exchange (where b and $d(s)$ are down type quarks). The dimensionless coupling constant $A^{bd(s)}_{\alpha\alpha}$ is given by

$$A^{bd(s)}_{\alpha\alpha} = \frac{\sqrt{2}}{4G_F}\sum_{k=1}^{3}\frac{\lambda'_{\alpha k1(2)}\lambda'^*_{\alpha k3}}{2m^2_{\tilde{d}^c_k}}. \quad (10)$$

The differential decay rate for semileptonic decay processes is given by [62–64]

$$\frac{d\Gamma}{dq^2} = \frac{1}{2^5\pi^5}\lambda^{3/2}\left(1, r, s\right) m_B^3 \left|f_p^+\left(q^2\right)\right|^2 \left|C_l\right|^2, \quad (11)$$

where

$$C_l = C_{SM} + \frac{z}{8}e^{i\theta}, \quad (12)$$

with

$$C_{SM} = \frac{G_F\alpha}{2\sqrt{2}\sin^2\theta_w}\left(V^*_{cb}V_{cd(s)}X^l_{NL} + V^*_{tb}V_{td(s)}X\left(x_t\right)\right), \quad (13)$$

with

$$\begin{aligned} X\left(x_t\right) &= X_0\left(x_t\right) + \frac{\alpha_S}{4\pi}X_l\left(x_t\right), \\ x_t &= \frac{\overline{m}_t^2\left(\mu_t\right)}{M_W^2}, \\ \mu_t &= O\left(m_t\right), \end{aligned} \quad (14)$$

and z as explained in the above section is the general NP parameter and $\lambda'_{\alpha k1(2)}\lambda'^*_{\alpha k3}/m^2_{\tilde{d}^c_k}$. We have used the form factor $f_p^+(q^2)$ for the above decay processes of $B- > \pi(K)$ as given in [67]. The decay rate for pure leptonic decay processes is given by [46, 50–52]

$$\Gamma\left(b \longrightarrow d\left(s\right)\nu_l\overline{\nu}_l\right) = \frac{1}{8\pi}m_B^3\left|f_P\left(q^2\right)\right|^2\left|\frac{2m_l}{m_B}C_l\right|^2. \quad (15)$$

The form factor $f_p(q^2)$ is given by [66], m_B represents the mass of beauty meson and m_l is the mass of lepton.

4. Results and Discussions

We have carried out study of hypercharge changing two and three body decay processes of pseudoscalar mesons ($M \longrightarrow X\nu_\alpha\overline{\nu}_\alpha$; $M \longrightarrow \nu_\alpha\overline{\nu}_\alpha$), where $M = K, B$; $\alpha = e, \mu, \tau$ and $X = \pi, K$. This study considers two types of processes: polarized and unpolarized flavor of the lepton. The analysis carried out involves comparison of branching fraction of a certain decay process (mentioned above) calculated from both theoretical and experimental ground. This comparison not only helps to place bounds (listed in Tables 2, 4, and 5) on $\not{R}_p$ Yukawa couplings $\lambda'_{\alpha k\beta}\lambda'^*_{\alpha k\gamma}$ but also enables to predict (listed in Tables 3, 6–9) the enhancement of similar processes (having identical FCNC). The enhancement is given in three forms, namely, NP (contribution from Yukawa couplings only), Interference (product of SM contribution, coming from C_{SM} and Yukawa couplings), and combined (NP+Interference). All the results are displayed in graphs plotted in Figures 2–13, which are composed of simple (variation of branching fraction with respect to the magnitude of NP parameter, i.e., $|z(\lambda'_{\rho\omega\sigma}\lambda'^*_{\alpha\beta\gamma})|$) and contour plot (region plot of magnitude and phase of NP parameter at different values of branching fraction within limits of experimental measurements). A visual error analysis for the experimental measurement of branching fraction is also presented in these graphs by constraining lines at mean and $\pm1\sigma$ level. Similar error analysis is repeated in tables. The Feynman diagrams and table listing experimental data [68] related to these processes are given in Figure 1 and Table 1, respectively. The Yukawa couplings ($\lambda'_{\rho\omega\sigma}\lambda'^*_{\alpha\beta\gamma}$) involved are normalized to the square of $m_{\overline{d}^c}/100\,GeV$ in all these tables and figures.

First, we will discuss the results related to semileptonic decay processes followed by pure leptonic decays. We have plotted graphs in Figures 2 and 3 for the study of process $K \longrightarrow \pi\nu_\alpha\overline{\nu}_a$. These plots relate the branching fraction of the said process with the magnitude and phase of NP parameters ($|z(\lambda'_{ik1}\lambda'^*_{ik2})|$ and θ). Contour plots in Figure 2 represent the allowed region for NP parameters (magnitude and phase) for specific values of branching fraction. All four plots (comprising unpolarized (a) and polarized (b-d)) show that the maximum magnitude of NP parameter oscillates with respect to its phase in general. The plot in Figure 2(a) shows a particular pattern at given error, i.e., at -1σ level of measured branching fraction (0.7×10^{-7}). It clearly shows that only a narrow range of phase of NP parameter ($|\theta| \leq \pi/4$) is allowed for given -1σ level. The bounds on the magnitude

Table 1: Table listing the properties of processes under discussion [68]. Here $|z|$ is the strength of the NP parameter.

Process	Experimental Measurement	SM Prediction	Bounds on New Physics Parameter	
			Magnitude $\lvert z\rvert$	Phase (θ)
$B \longrightarrow \pi\nu\bar{\nu}$	$< 9.8 \times 10^{-5}$	1.62×10^{-7}	$< 1.79 \times 10^{-6}$	$\leq 2\pi$
$B_d^0 \longrightarrow \nu\bar{\nu}$		$6.13 \times 10^{-31}(e)$ $4.57 \times 10^{-27}(\mu)$ $5.91 \times 10^{-25}(\tau)$		$\leq 2\pi$
$B \longrightarrow K\nu\bar{\nu}$	$< 1.6 \times 10^{-5}$	4.40×10^{-4}	$< 8.69 \times 10^{-7}$	$\leq 2\pi$
$B_s^0 \longrightarrow \nu\bar{\nu}$		$1.36 \times 10^{-29}(e)$ $1.02 \times 10^{-25}(\mu)$ $1.32 \times 10^{-23}(\tau)$		$\leq 2\pi$
$K^{\pm} \longrightarrow \pi\nu\bar{\nu}$	$< (1.7 \pm 1.0) \times 10^{-5}$	8.23×10^{-11}	$(7.83 \pm 2.01) \times 10^{-9}(e)$ $(7.83 \pm 2.01) \times 10^{-9}(\mu)$ $(7.81 \pm 2.01) \times 10^{-9}(\tau)$	$\leq 2\pi$
$K_s^0 \longrightarrow \nu\bar{\nu}$		$7.24 \times 10^{-33}(e)$ $5.40 \times 10^{-29}(\mu)$ $6.98 \times 10^{-27}(\tau)$		$\leq 2\pi$
$K_L^0 \longrightarrow \nu\bar{\nu}$		$4.27 \times 10^{-33}(e)$ $3.19 \times 10^{-29}(\mu)$ $4.06 \times 10^{-27}(\tau)$		$\leq 2\pi$
$K^0 \longrightarrow \pi^0\nu\bar{\nu}$ (Bounds on New Physics parameters have been calculated numerically for their fit with SM prediction)	$< 2.6 \times 10^{-5}$	2.76×10^{-11}	$< 1.9 \times 10^{-9}$ $< 9.83 \times 10^{-10}$ $< 6.96 \times 10^{-10}$ $< 5.68 \times 10^{-10}$ $< 5.09 \times 10^{-10}$ $< 4.92 \times 10^{-10}$	15° 30° 45° 60° 75° 90°

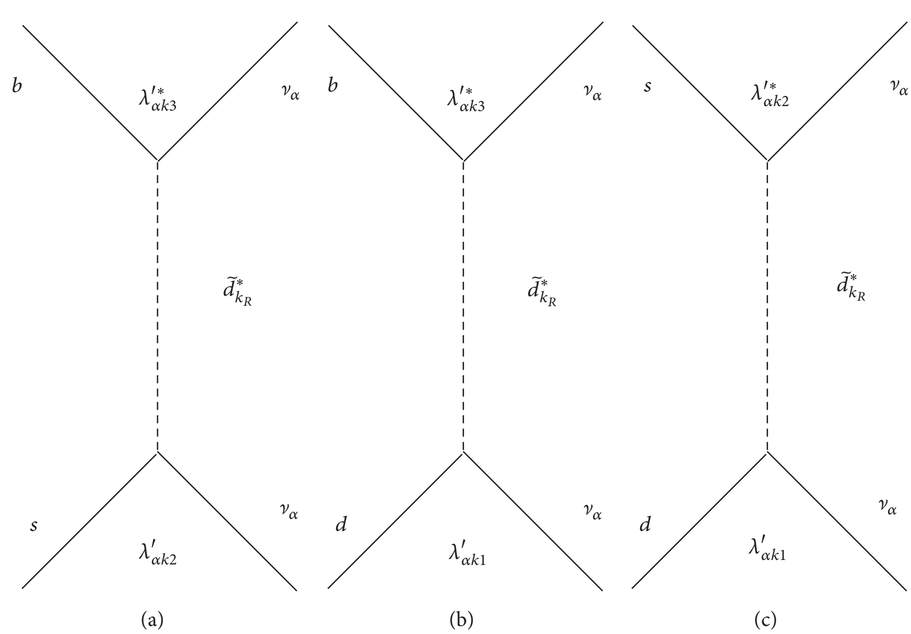

Figure 1: Feynman diagrams of (a) $b \longrightarrow s\nu_\alpha\bar{\nu}_\alpha$, (b) $b \longrightarrow d\nu_\alpha\bar{\nu}_\alpha$, (c) $s \longrightarrow d\nu_\alpha\bar{\nu}_\alpha$. $\alpha = 1, 2, 3$.

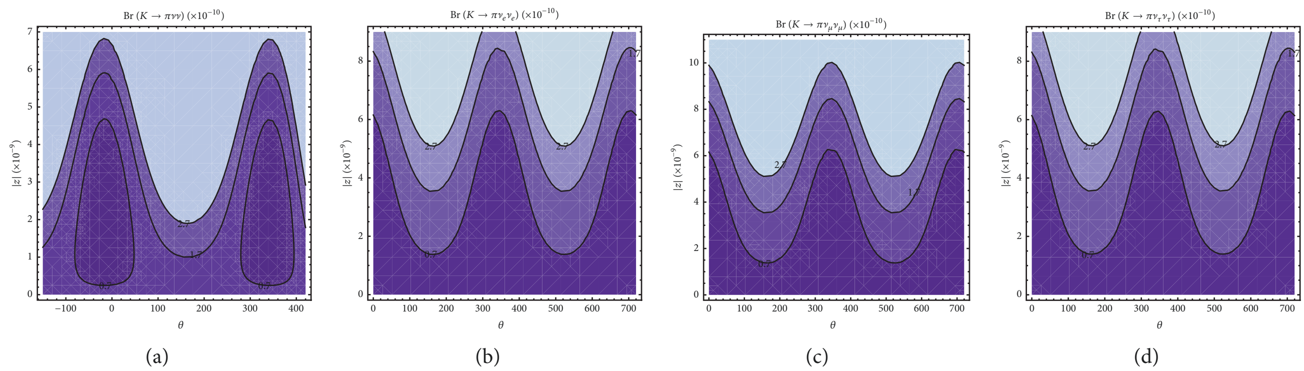

FIGURE 2: Allowed region of general NP parameters (z, θ) for $K \longrightarrow \pi \nu_\alpha \overline{\nu}_\alpha$ at several values of branching fraction. α is (a) unpolarized, (b) e, (c) μ, (d) τ. The three contours belong to branching fraction at $[0.7, 1.7, 2.7] \times 10^{-10}$.

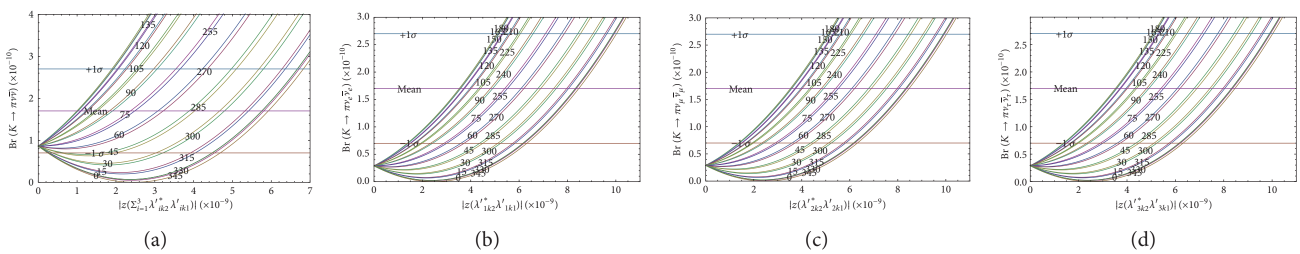

FIGURE 3: Variations of branching fraction w.r.t NP parameter $|z(\lambda'_{ijk}\lambda'_{lmn})|$ at several values of θ for $K \longrightarrow \pi \nu_\alpha \overline{\nu}_\alpha$. α is (a) unpolarized, (b) e, (c) μ, (d) τ. The three bounds belong to branching fraction at $[0.7\ (-1\sigma), 1.7\ (Mean), 2.7\ (+1\sigma)] \times 10^{-10}$ corresponding to an experimental measurement of $(1.7 \pm 0.7) \times 10^{-10}$.

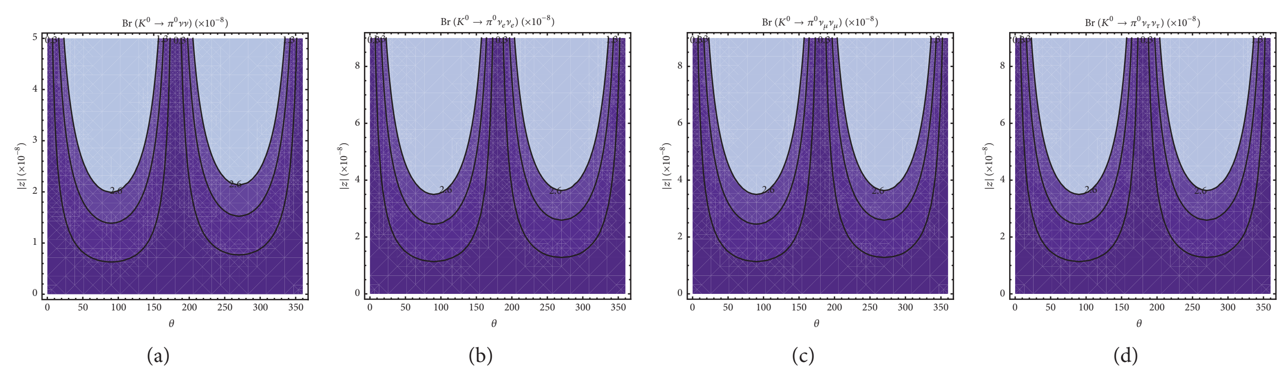

FIGURE 4: Allowed regions of general NP parameters (z, θ) for $K^0 \longrightarrow \pi^0 \nu_\alpha \overline{\nu}_\alpha$ at specific values of branching fraction. α is (a) unpolarized, (b) e, (c) μ, (d) τ. The three contours belong to branching fraction at $[0.3, 1.3, 2.6] \times 10^{-8}$.

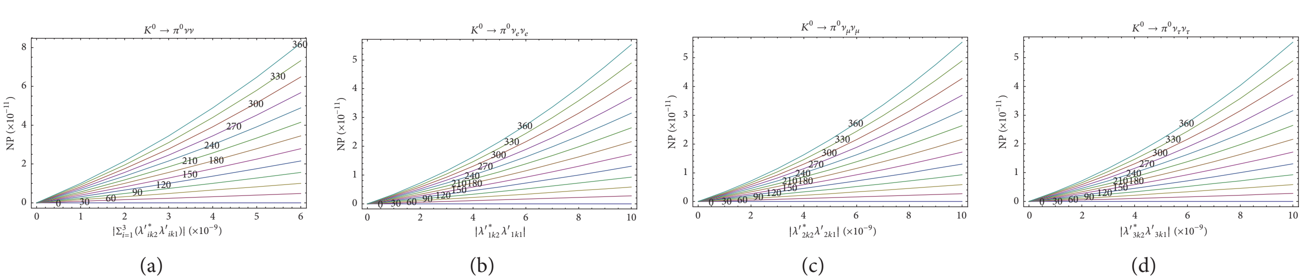

FIGURE 5: Variations of branching fraction (NP contribution only) with respect to NP parameter $|\lambda'_{ijk}\lambda'_{lmn}|$ at several values of θ for $K^0 \longrightarrow \pi^0 \nu_\alpha \overline{\nu}_\alpha$. α is (a) unpolarized, (b) e, (c) μ, (d) τ.

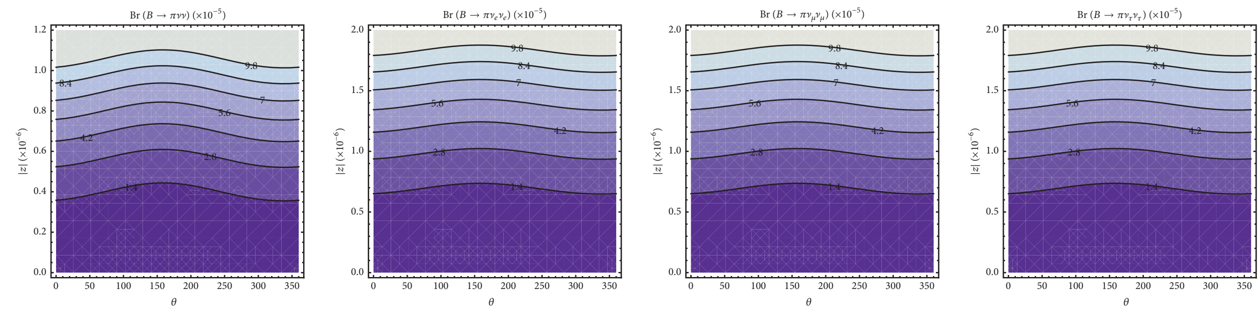

(a) (b) (c) (d)

Figure 6: Allowed regions of general NP parameters (z, θ) for $B \longrightarrow \pi\nu_\alpha\overline{\nu}_\alpha$ at specific values of branching fraction. α is (a) unpolarized, (b) e, (c) μ, (d) τ. The three contours belong to branching fraction at $[1.4 - 9.8] \times 10^{-6}$.

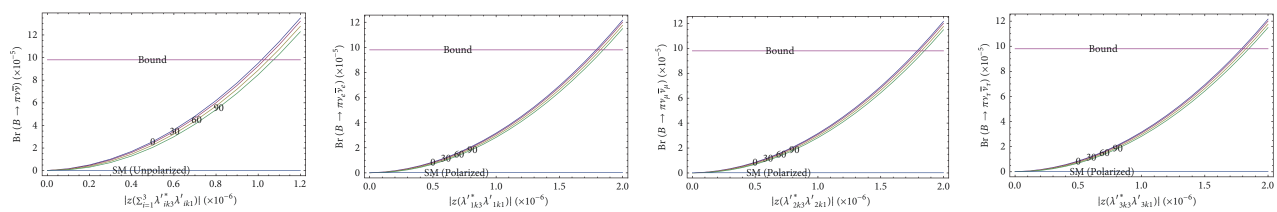

(a) (b) (c) (d)

Figure 7: Variation of branching fraction with respect to NP parameter $|z(\lambda'_{ijk}\lambda'_{lmn})|$ at several values of θ for $B \longrightarrow \pi\nu_\alpha\overline{\nu}_\alpha$. α is (a) unpolarized, (b) e, (c) μ, (d) τ. Experimental bound on the process is 9.8×10^{-5}.

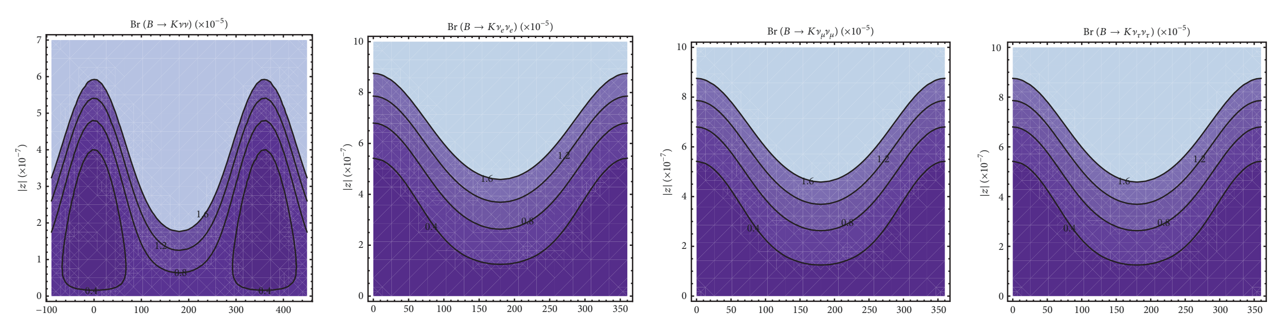

(a) (b) (c) (d)

Figure 8: Allowed regions of general NP parameters (z, θ) for $B \longrightarrow K\nu_\alpha\overline{\nu}_\alpha$ at specific values of branching fraction. α is (a) unpolarized, (b) e, (c) μ, (d) τ. The three contours belong to branching fraction at $[0.4 - 1.6] \times 10^{-5}$.

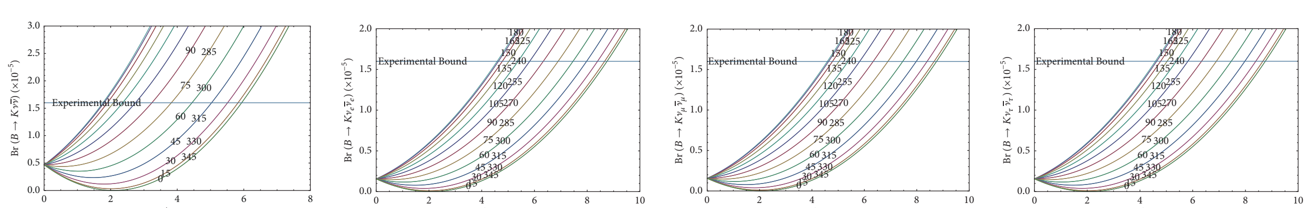

(a) (b) (c) (d)

Figure 9: Variations of branching fraction with respect to NP parameter $|z(\lambda'_{ijk}\lambda'_{lmn})|$ at several values of θ for $B \longrightarrow K\nu_\alpha\overline{\nu}_\alpha$. α is (a) unpolarized, (b) e, (c) μ, (d) τ. Experimental bound on the process is 1.6×10^{-5}.

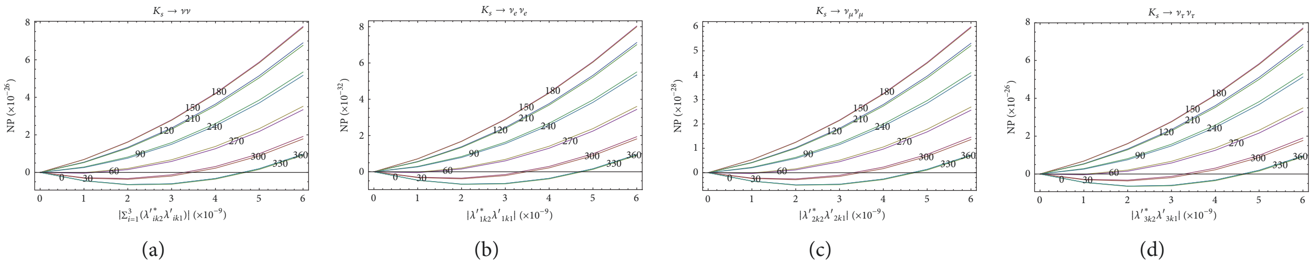

FIGURE 10: Variations of branching fraction (NP contribution only) with respect to NP parameter $|\lambda'_{ijk}\lambda'_{lmn}|$ at several values of θ for $K_S \longrightarrow \nu_\alpha\overline{\nu}_\alpha$. α is (a) unpolarized, (b) e, (c) μ, (d) τ.

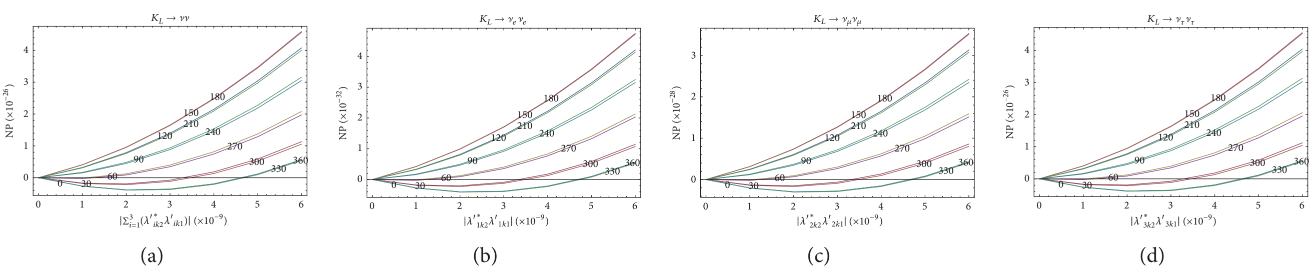

FIGURE 11: Variations of branching fraction (NP contribution only) with respect to NP parameter $|\lambda'_{ijk}\lambda'_{lmn}|$ at several values of θ for $K_L \longrightarrow \nu_\alpha\overline{\nu}_\alpha$. α is (a) unpolarized, (b) e, (c) μ, (d) τ.

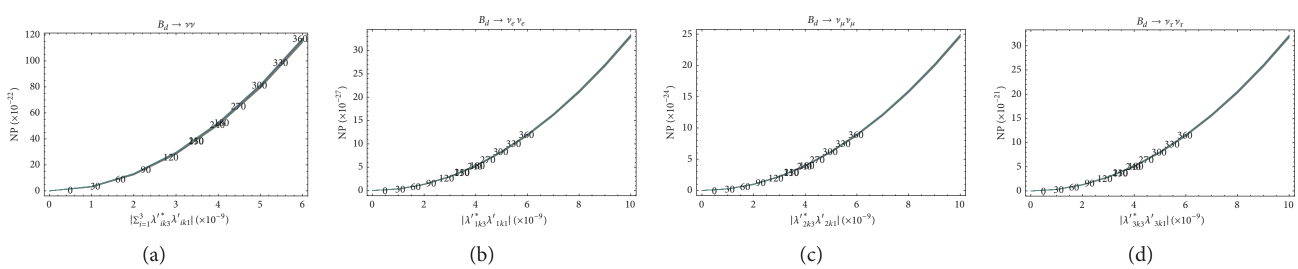

FIGURE 12: Variations of branching fraction (NP contribution only) with respect to NP parameter $|\lambda'_{ijk}\lambda'_{lmn}|$ at several values of θ for $B_d \longrightarrow \nu_\alpha\overline{\nu}_\alpha$. α is (a) unpolarized, (b) e, (c) μ, (d) τ.

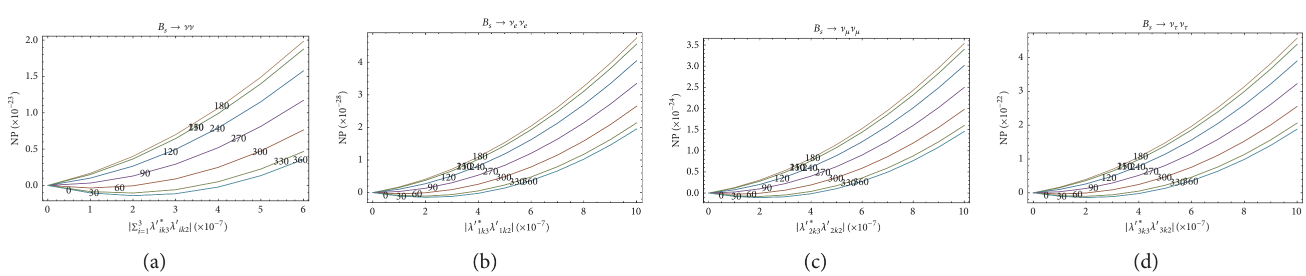

FIGURE 13: Variations of branching fraction (NP contribution only) with respect to NP parameter $|\lambda'_{ijk}\lambda'_{lmn}|$ at several values of θ for $B_s \longrightarrow \nu_\alpha\overline{\nu}_\alpha$. α is (a) unpolarized, (b) e, (c) μ, (d) τ.

Table 2: Bounds on NP parameters ($|z(\lambda'_{ijk}\lambda'_{lmn})|,\theta$) for $K \longrightarrow \pi\nu_\alpha\overline{\nu}_\alpha$. α (Br_{SM}) is (a) unpolarized (8.63×10^{-11}), (b) e (2.89×10^{-11}),(c) μ (2.89×10^{-11}), (d) τ (2.85×10^{-11}). Experimental limits are $(1.7 \pm 1.0) \times 10^{-10}$.

(a)

Bounds on NP Parameter (unpolarized)	
θ	$\lvert z(\Sigma_{i=1}^{3}\lambda'^{\star}_{ik2}\lambda'_{ik1})\rvert \times 10^{-9}$
0	3.465 ± 3.209
30	3.032 ± 2.653
60	4.229 ± ....
90	2.972 ± ....
120	2.233 ± ....
150	1.927 ± ....
180	1.94 ± ....
210	2.278 ± ....
240	3.062 ± ....
270	4.357 ± ....
300	3.078 ± 2.721
330	3.486 ± 3.233
360	3.465 ± 3.209

(b)

Bounds on NP Parameter (unpolarized)	
θ	$\lvert z(\Sigma_{i=1}^{3}\lambda'^{\star}_{ik2}\lambda'_{ik1})\rvert \times 10^{-9}$
0	5.575 ± 1.098
30	4.356 ± 1.328
60	4.229 ± ....
90	2.972 ± ....
120	2.233 ± ....
150	1.927 ± ....
180	1.94 ± ....
210	2.278 ± ....
240	3.062 ± ....
270	4.357 ± ....
300	4.504 ± 1.295
330	5.629 ± 1.09
360	5.575 ± 1.098

(c)

Bounds on NP Parameter	
θ	$\lvert z(\lambda'^{\star}_{1k2}\lambda'_{1k1})\rvert \times 10^{-9}$
0	8.026 ± 1.87
30	7.083 ± 1.967
60	5.671 ± 2.079
90	4.408 ± 2.072
120	3.618 ± 1.956
150	3.267 ± 1.865
180	3.282 ± 1.87

(c) Continued.

Bounds on NP Parameter	
θ	$\lvert z(\lambda'^{\star}_{1k2}\lambda'_{1k1})\rvert \times 10^{-9}$
210	3.666 ± 1.967
240	4.498 ± 2.079
270	5.793 ± 2.072
300	7.189 ± 1.956
330	8.068 ± 1.865
360	8.026 ± 1.87

(d)

Bounds on NP Parameter	
θ	$\lvert z(\lambda'^{\star}_{2k2}\lambda'_{2k1})\rvert \times 10^{-9}$
0	8.026 ± 1.87
30	7.083 ± 1.967
60	5.671 ± 2.079
90	4.409 ± 2.072
120	3.618 ± 1.956
150	3.267 ± 1.865
180	3.282 ± 1.87
210	3.666 ± 1.967
240	4.499 ± 2.079
270	5.793 ± 2.072
300	7.189 ± 1.956
330	8.068 ± 1.865
360	8.026 ± 1.87

(e)

Bounds on NP Parameter	
θ	$\lvert z(\lambda'^{\star}_{3k2}\lambda'_{3k1})\rvert \times 10^{-9}$
0	8.009 ± 1.87
30	7.071 ± 1.966
60	5.671 ± 2.076
90	4.418 ± 2.069
120	3.631 ± 1.954
150	3.282 ± 1.865
180	3.298 ± 1.87
210	3.684 ± 1.966
240	4.515 ± 2.076
270	5.803 ± 2.069
300	7.186 ± 1.954
330	8.054 ± 1.865
360	8.009 ± 1.87

of NP parameter are given in Table 2. Here the entry "±......." means that these specific NP parameters cannot be defined

Table 3: Bounds on NP parameters ($|\lambda'_{ijk}\lambda'_{lmn}|$,$\theta$) derived from $K \longrightarrow \pi\nu_\alpha\overline{\nu}_\alpha$ for $K^0 \longrightarrow \pi^0\nu_\alpha\overline{\nu}_\alpha$. α (Br_{SM}) is (a) unpolarized ($2.94. \times 10^{-11}$) and 9.78×10^{-12} for (b) e, (c) μ, (d) τ. Experimental bound on the process is 2.6×10^{-8}.

(a)

	Bounds on NP Parameter	Branching Fraction ($\times 10^{-10}$)		
θ	$\lvert\Sigma_{i=1}^{3}(\lambda'^{\star}_{ik2}\lambda'_{ik1})\rvert \times 10^{-9}$	NP	Interference	Combined
0	3.465 ± 3.209	0. ± 0.	0. ± 0.	0.003 ± 0.
30	3.032 ± 2.653	2.484 ± 2.462	−2.446 ± 2.426	0.041 ± 0.036
60	4.229 ±	8.212 ±	−8.099 ±	0.116 ± ....
90	2.972 ±	5.407 ±	−5.328 ±	0.082 ± ....
120	2.233 ±	2.289 ±	−2.25 ±	0.042 ± ....
150	1.927 ±	0.568 ±	−0.555 ±	0.017 ± ....
180	1.94 ±	0 ±	0 ±	0.003 ± ....
210	2.278 ±	0.794 ±	−0.796 ±	0.001 ± ....
240	3.062 ±	4.304 ±	−4.283 ±	0.023 ± ....
270	4.357 ±	11.621 ±	−11.541 ±	0.082 ± ....
300	3.078 ± 2.721	7.75 ± 7.691	−7.695 ± 7.634	0.058 ± 0.057
330	3.486 ± 3.233	3.46 ± 3.45	−3.44 ± 3.429	0.023 ± 0.021
360	3.465 ± 3.209	0. ± 0.	0. ± 0.	0.003 ± 0.

(b)

	Bounds on NP Parameter	Branching Fraction ($\times 10^{-10}$)		
θ	$\lvert\lambda'^{\star}_{1k2}\lambda'_{1k1}\rvert \times 10^{-9}$	NP	Interference	Combined
0	8.026 ± 1.87	0. ± 0.	0. ± 0.	0.001 ± 0.
30	7.083 ± 1.967	2.757 ± 1.422	−2.719 ± 1.405	0.039 ± 0.017
60	5.671 ± 2.079	5.585 ± 3.609	−5.515 ± 3.568	0.071 ± 0.041
90	4.408 ± 2.072	4.843 ± 3.729	−4.782 ± 3.686	0.062 ± 0.043
120	3.618 ± 1.956	2.589 ± 2.166	−2.554 ± 2.14	0.036 ± 0.026
150	3.267 ± 1.865	0.722 ± 0.622	−0.71 ± 0.613	0.013 ± 0.009
180	3.282 ± 1.87	0. ± 0.	0. ± 0.	0.001 ± 0.
210	3.666 ± 1.967	0.883 ± 0.736	−0.879 ± 0.731	0.005 ± 0.005
240	4.498 ± 2.079	3.759 ± 2.863	−3.732 ± 2.839	0.028 ± 0.024
270	5.793 ± 2.072	7.726 ± 4.9	−7.665 ± 4.857	0.062 ± 0.043
300	7.189 ± 1.956	8.497 ± 4.306	−8.429 ± 4.267	0.068 ± 0.038
330	8.068 ± 1.865	3.499 ± 1.536	−3.475 ± 1.523	0.025 ± 0.013
360	8.026 ± 1.87	0. ± 0.	0. ± 0.	0.001 ± 0.

(c)

	Bounds on NP Parameter	Branching Fraction ($\times 10^{-10}$)		
θ	$\lvert\lambda'^{\star}_{2k2}\lambda'_{2k1}\rvert \times 10^{-9}$	NP	Interference	Combined
0	8.026 ± 1.87	0. ± 0.	0. ± 0.	0.001 ± 0.
30	7.083 ± 1.967	2.757 ± 1.422	−2.719 ± 1.405	0.039 ± 0.017
60	5.671 ± 2.079	5.585 ± 3.609	−5.515 ± 3.568	0.071 ± 0.041
90	4.409 ± 2.072	4.843 ± 3.729	−4.782 ± 3.686	0.062 ± 0.043
120	3.618 ± 1.956	2.589 ± 2.167	−2.554 ± 2.14	0.036 ± 0.026
150	3.267 ± 1.865	0.722 ± 0.622	−0.71 ± 0.613	0.013 ± 0.009
180	3.282 ± 1.87	0. ± 0.	0. ± 0.	0.001 ± 0.
210	3.666 ± 1.967	0.883 ± 0.736	−0.88 ± 0.731	0.005 ± 0.005
240	4.499 ± 2.079	3.759 ± 2.863	−3.732 ± 2.839	0.028 ± 0.024
270	5.793 ± 2.072	7.726 ± 4.9	−7.665 ± 4.857	0.062 ± 0.043
300	7.189 ± 1.956	8.496 ± 4.305	−8.429 ± 4.267	0.068 ± 0.038

(c) Continued.

θ	Bounds on NP Parameter $\lvert\lambda'^{*}_{2k2}\lambda'_{2k1}\rvert \times 10^{-9}$	Branching Fraction ($\times 10^{-10}$) NP	Interference	Combined
330	8.068 ± 1.865	3.498 ± 1.536	−3.475 ± 1.523	0.025 ± 0.013
360	8.026 ± 1.87	0. ± 0.	0. ± 0.	0.001 ± 0.

(d)

θ	Bounds on NP Parameter $\lvert\lambda'^{*}_{3k2}\lambda'_{3k1}\rvert \times 10^{-9}$	Branching Fraction ($\times 10^{-10}$) NP	Interference	Combined
0	8.009 ± 1.87	0. ± 0.	0. ± 0.	0.001 ± 0.
30	7.071 ± 1.966	2.748 ± 1.418	−2.711 ± 1.401	0.038 ± 0.017
60	5.671 ± 2.076	5.582 ± 3.603	−5.513 ± 3.562	0.071 ± 0.041
90	4.418 ± 2.069	4.856 ± 3.73	−4.795 ± 3.687	0.062 ± 0.043
120	3.631 ± 1.954	2.603 ± 2.173	−2.568 ± 2.146	0.036 ± 0.027
150	3.282 ± 1.865	0.727 ± 0.625	−0.715 ± 0.616	0.013 ± 0.009
180	3.298 ± 1.87	0. ± 0.	0. ± 0.	0.001 ± 0.
210	3.684 ± 1.966	0.89 ± 0.739	−0.886 ± 0.734	0.005 ± 0.005
240	4.515 ± 2.076	3.78 ± 2.869	−3.753 ± 2.845	0.028 ± 0.024
270	5.803 ± 2.069	7.745 ± 4.899	−7.684 ± 4.856	0.062 ± 0.043
300	7.186 ± 1.954	8.488 ± 4.299	−8.421 ± 4.261	0.068 ± 0.038
330	8.054 ± 1.865	3.487 ± 1.533	−3.464 ± 1.52	0.024 ± 0.013
360	8.009 ± 1.87	0. ± 0.	0. ± 0.	0.001 ± 0.

for -1σ as the corresponding $R\!\!\!/_p$ MSSM contribution exceeds the experimental limit on branching fraction in -1σ error. Tables 2(a) and 2(b) show the same pattern as observed in Figures 2(a) and 3(a) numerically. Since Yukawa couplings for R-parity violation are identical for the processes ($K \longrightarrow \pi\nu_\alpha\overline{\nu}_\alpha, K^0 \longrightarrow \pi^0\nu_\alpha\overline{\nu}_\alpha, K_{L,S} \longrightarrow \nu_\alpha\overline{\nu}_\alpha$), the maximum limits for $K \longrightarrow \pi\nu_\alpha\overline{\nu}_\alpha$ are used for calculating NP contribution to branching fraction of other processes. Figure 3 represent the variation of branching fraction with respect to the magnitude of NP parameter at several values of its phase θ.

Contour plots in Figure 4 represent the allowed region for NP parameters ($|z(\lambda'_{ik1}\lambda'^{*}_{ik2})|$ and θ) for specific values of branching fraction of the process $K^0 \longrightarrow \pi^0\nu_\alpha\overline{\nu}_a$. All four plots (comprising unpolarized (a) and polarized (b-d)) show that the maximum magnitude of NP parameter follows a *catenary* (hanging chain) pattern, with the bottom level smoothening with decreasing error levels. The bounds on the magnitude of NP parameter and possible NP contribution are in Table 3, which shows that $R\!\!\!/_p$ MSSM dominates over SM contribution by order of magnitude ~10^2, but the overall effect is to give a comparatively less contribution due to destructive interference. The plots in Figure 5 represent the variation of branching fraction (NP contribution only) for the process $K^0 \longrightarrow \pi^0\nu_\alpha\overline{\nu}_a$ with respect to the magnitude of NP parameter at several values of its phase θ.

Contour graphs in Figure 6 illustrate the allowed region for NP parameters ($|z(\lambda'_{ik1}\lambda'^{*}_{ik3})|$ and θ) of the process $B \longrightarrow \pi\nu_\alpha\overline{\nu}_a$ for specific values of branching fraction. All four plots (comprising unpolarized (a) and (b-d)) show that the maximum magnitude of NP parameter oscillates gently with respect to its phase in general. Similarly, plots in Figure 7 represent the variation of branching fraction with respect to the magnitude of NP parameter ($|z(\lambda'_{ik1}\lambda'^{*}_{ik3})|$) at several values of its phase θ. All four plots demonstrate the gentle oscillation behavior as observed in Figure 6 with sharply distinct curves for different values of phases of NP parameter θ. The bounds on the magnitude of NP parameter are given in Table 4.

Contour graphs in Figure 8 depict the allowed region for NP parameters ($|z(\lambda'_{ik3}\lambda'^{*}_{ik2})|$ and θ) of the process $B \longrightarrow K\nu_\alpha\overline{\nu}_a$ for specific values of branching fraction bounded by the experimental limit, while plots in Figure 9 represent the variation of branching fraction of the process $B \longrightarrow K\nu_\alpha\overline{\nu}_a$ with the magnitude of NP parameters at several values of its phase θ. All four plots (comprising unpolarized (a) and polarized (b-d)) show that the maximum magnitude of NP parameter oscillates with respect to its phase in general. The plot in Figure 8(a) shows a particular pattern below given limiting branching fraction ($\leq 4 \times 10^{-6}$). This particular pattern shows that only a narrow range of phase θ of NP parameter is allowed in that case. The bounds on the magnitude of NP parameter are given in Table 5.

Table 4: Bounds on NP parameters ($|z(\lambda'_{ijk}\lambda'_{lmn})|,\theta$) for $B \longrightarrow \pi\nu_\alpha\overline{\nu}_\alpha$. α (Br_{SM}) is (a) unpolarized (1.73×10^{-7}) and 5.76×10^{-8} for (b) e, (c) μ, (d) τ. Experimental bound on the process is 9.8×10^{-5}.

(a)

Bounds on NP Parameter (unpolarized)	
θ	$\|z(\Sigma_{i=1}^{3}\lambda'^{\star}_{ik3}\lambda'_{ik1})\|\times10^{-6}$
0	1.0164
30	1.0298
60	1.0506
90	1.0735
120	1.0923
150	1.1016
180	1.0987
210	1.0844
240	1.0629
270	1.0402
300	1.0223
330	1.0137
360	1.0164

(b)

Bounds on NP Parameter	
θ	$\|z(\lambda'^{\star}_{1k3}\lambda'_{1k1})\|\times10^{-6}$
0	1.7907
30	1.8043
60	1.8252
90	1.8481
120	1.8667
150	1.8759
180	1.873
210	1.8589
240	1.8376
270	1.8148
300	1.7967
330	1.7879
360	1.7907

(c)

Bounds on NP Parameter	
θ	$\|z(\lambda'^{\star}_{2k3}\lambda'_{2k1})\|\times10^{-6}$
0	1.7907
30	1.8043
60	1.8252
90	1.8481
120	1.8667
150	1.8759
180	1.873
210	1.8589
240	1.8376

(c) Continued.

Bounds on NP Parameter	
θ	$\|z(\lambda'^{\star}_{2k3}\lambda'_{2k1})\|\times10^{-6}$
270	1.8148
300	1.7967
330	1.7879
360	1.7907

(d)

Bounds on NP Parameter	
θ	$\|z(\lambda'^{\star}_{3k3}\lambda'_{1k1})\|\times10^{-6}$
0	1.7907
30	1.8043
60	1.8252
90	1.8481
120	1.8667
150	1.8759
180	1.873
210	1.8589
240	1.8376
270	1.8148
300	1.7967
330	1.7879
360	1.7907

Table 5: Bounds on NP parameters ($|z(\lambda'_{ijk}\lambda'_{lmn})|,\theta$) for $B \longrightarrow K\nu_\alpha\overline{\nu}_\alpha$. α (Br_{SM}) is (a) unpolarized (4.69×10^{-6}) and (1.56×10^{-6}) for (b) e, (c) μ, (d) τ. Experimental bound on the process is 1.6×10^{-5}.

(a)

Bounds on NP Parameter (unpolarized)	
θ	$\|z(\Sigma_{i=1}^{3}\lambda'^{\star}_{ik3}\lambda'_{ik2})\|\times10^{-7}$
0	5.9349
30	5.512
60	4.4436
90	3.238
120	2.3595
150	1.9022
180	1.7667
210	1.9022
240	2.3595
270	3.238
300	4.4436
330	5.512
360	5.9349

(b)

Bounds on NP Parameter	
θ	$\|z(\lambda'^{\star}_{1k3}\lambda'_{1k2})\|\times10^{-7}$
0	8.7538
30	8.3927

(b) Continued.

θ	Bounds on NP Parameter $\vert z(\lambda'^{*}_{1k3}\lambda'_{1k2})\vert \times 10^{-7}$
60	7.4629
90	6.3358
120	5.3788
150	4.7829
180	4.5856
210	4.7829
240	5.3788
270	6.3358
300	7.4629
330	8.3927
360	8.7538

(c)

θ	Bounds on NP Parameter $\vert z(\lambda'^{*}_{2k3}\lambda'_{2k2})\vert \times 10^{-7}$
0	8.7538
30	8.3927
60	7.4629
90	6.3358
120	5.3788
150	4.7829
180	4.5856
210	4.7829
240	5.3788
270	6.3358
300	7.4629
330	8.3927
360	8.7538

(d)

θ	Bounds on NP Parameter $\vert z(\lambda'^{*}_{3k3}\lambda'_{3k2})\vert \times 10^{-7}$
0	8.7539
30	8.3927
60	7.4629
90	6.3357
120	5.3788
150	4.7829
180	4.5856
210	4.7829
240	5.3788
270	6.3357
300	7.4629
330	8.3927
360	8.7539

Plots in Figures 10 and 11 of the process $K_{L,S} \longrightarrow \nu_\alpha\overline{\nu}_\alpha$ display the variation of branching fraction (NP contribution only) with respect to the magnitude of NP parameter at several values of its phase θ. For pure leptonic decays of strange mesons involving neutrinos ($K_{L,S} \longrightarrow \nu_\alpha\overline{\nu}_\alpha$), there is no experimental data available. Therefore, we use limits derived from $K \longrightarrow \pi\nu_\alpha\overline{\nu}_\alpha$ to calculate NP contribution to these processes. The bounds on the magnitude of NP parameter and possible NP contribution are given in Tables 6 and 7 for the decay of $K_{L,S}$, respectively, which shows that $\not{R}_p$ MSSM enhances SM contribution by order of 10 for $K_{L,S}$. The interference term in this case is both constructive and destructive, but the destructive effect is not strong enough to affect the enhancement by SUSY.

Plots in Figures 12 and 13 describe the variation of branching fraction (NP contribution only) of the process $B_{s,d} \longrightarrow \nu_\alpha\overline{\nu}_\alpha$ with the magnitude of NP parameters, $(|z(\lambda'_{ik1}\lambda'^{*}_{ik3})|$ at several values of θ. For pure leptonic decays of beauty involving neutrinos ($B_{s,d} \longrightarrow \nu_\alpha\overline{\nu}_\alpha$), there is no experimental data available for these processes, and we use limits derived from $B \longrightarrow (\pi, K)\nu_\alpha\overline{\nu}_\alpha$ to calculate NP contributions to these processes. The bounds on the magnitude of NP parameter and possible NP contribution are given in Tables 8 and 9, respectively for the decay of $B_{s,d}$, which shows that $\not{R}_p$ MSSM enhances SM contribution by order of magnitude 10 for B_s and 10^4 for B_d and also the effect of destructive interference is not strong to affect SUSY enhancement.

5. Summary and Conclusion

Summarizing, we have carried out an analysis of semileptonic ($M \longrightarrow M'\nu_a\overline{\nu}_\alpha; M = K, B;\ M' = \pi, K; \alpha = e, \mu, \tau$) and pure leptonic ($M \longrightarrow \nu_\alpha\overline{\nu}_\alpha$) decays of pseudoscalar mesons within the framework of $\not{R}_p$ MSSM. The analysis involves a detailed comparison of experimental results with respect to the theoretical prediction of the branching fraction of given processes. The comparison (listed in Tables 2–9) quantifies the effect of contribution from $\not{R}_p$ MSSM to the branching fraction of processes under discussion. The analysis performed (listed in Tables 3, 6–9) also enables to compare the branching fraction of processes having identical FCNC. The plots in Figures 2–13 show the variations of branching fraction with respect to NP parameters ($|z(\lambda'_{\alpha k\beta}\lambda'^{*}_{\alpha k\gamma})|$ and θ). In general, SM contribution is dominated by $\not{R}_p$ MSSM contribution, i.e., by a factor of 10 for the pure leptonic decays of $K_{L,S}$ and by 10^2 and 10^4 in case of B_s and B_d respectively. The interference term between $\not{R}_p$ MSSM and SM is both constructive and destructive but except for the semileptonic decays of K^0, it does not affect the enhancement due to SUSY. This makes $\not{R}_p$ MSSM a viable model for the comparison of NP contribution in rare decays at labs like Super B factories, KOTO (J-PARC) and NA62 at CERN.

Conflicts of Interest

The authors declare that there are no conflicts of interest.

TABLE 6: Bounds on NP parameters ($|\lambda'_{ijk}\lambda'_{lmn}|, \theta$) derived from $K \longrightarrow \pi\nu_\alpha\overline{\nu}_\alpha$ for $K_s \longrightarrow \nu_\alpha\overline{\nu}_\alpha$. α (Br_{SM}) is (a) unpolarized (7.27×10^{-27}), (b) e (7.58×10^{-33}), (c) μ (5.66×10^{-29}), (d) τ (7.27×10^{-27}).

(a)

	Bounds on NP Parameter		Branching Fraction ($\times 10^{-26}$)	
θ	$\lvert\Sigma_{i=1}^{3}(\lambda'^{*}_{ik2}\lambda'_{ik1})\rvert \times 10^{-9}$	NP	Interference	Combined
0	3.465 ± 3.209	2.69 ± 2.682	−1.952 ± 1.808	1.454 ± 0.873
30	3.032 ± 2.653	1.958 ± 1.94	−0.764 ± 0.669	1.91 ± 1.272
60	4.229 ±	2.157 ±	2.055 ±	4.928 ± ....
90	2.972 ±	1.065 ±	1.195 ±	2.976 ± ....
120	2.233 ±	0.601 ±	−0.808 ±	0.509 ± ....
150	1.927 ±	0.448 ±	−0.989 ±	0.175 ± ....
180	1.94 ±	0.454 ±	0.395 ±	1.565 ± ....
210	2.278 ±	0.626 ±	1.312 ±	2.654 ± ....
240	3.062 ±	1.131 ±	−0.079 ±	1.768 ± ....
270	4.357 ±	2.289 ±	−2.545 ±	0.46 ± ....
300	3.078 ± 2.721	2.035 ± 2.021	−0.476 ± 0.421	2.276 ± 1.6
330	3.486 ± 3.233	2.726 ± 2.718	1.87 ± 1.734	5.313 ± 4.453
360	3.465 ± 3.209	2.69 ± 2.682	1.109 ± 1.027	4.515 ± 3.709

(b)

	Bounds on NP Parameter		Branching Fraction ($\times 10^{-32}$)	
θ	$\lvert\lambda'^{*}_{1k2}\lambda'_{1k1}\rvert \times 10^{-9}$	NP	Interference	Combined
0	8.026 ± 1.87	8.435 ± 3.725	−4.716 ± 1.097	4.472 ± 2.628
30	7.083 ± 1.967	6.71 ± 3.46	−1.846 ± 0.513	5.618 ± 2.947
60	5.671 ± 2.079	4.53 ± 2.93	2.876 ± 1.052	8.16 ± 3.982
90	4.408 ± 2.072	2.95 ± 2.27	1.834 ± 0.862	5.538 ± 3.132
120	3.618 ± 1.956	2.1 ± 1.76	−1.368 ± 0.742	1.486 ± 1.018
150	3.267 ± 1.865	1.755 ± 1.515	−1.741 ± 0.997	0.768 ± 0.518
180	3.282 ± 1.87	1.77 ± 1.52	0.703 ± 0.403	3.227 ± 1.923
210	3.666 ± 1.967	2.15 ± 1.79	2.198 ± 1.18	5.102 ± 2.97
240	4.498 ± 2.079	3.05 ± 2.32	−0.131 ± 0.058	3.673 ± 2.262
270	5.793 ± 2.072	4.7 ± 2.98	−3.524 ± 1.259	1.93 ± 1.72
300	7.189 ± 1.956	6.895 ± 3.495	−1.145 ± 0.314	6.504 ± 3.181
330	8.068 ± 1.865	8.515 ± 3.735	4.513 ± 1.045	13.782 ± 4.78
360	8.026 ± 1.87	8.435 ± 3.725	2.66 ± 0.622	11.848 ± 4.347

(c)

	Bounds on NP Parameter		Branching Fraction ($\times 10^{-28}$)	
θ	$\lvert\lambda'^{*}_{2k2}\lambda'_{2k1}\rvert \times 10^{-9}$	NP	Interference	Combined
0	8.026 ± 1.87	6.29 ± 2.78	−3.497 ± 0.815	3.35 ± 1.964
30	7.083 ± 1.967	5.004 ± 2.58	−1.374 ± 0.381	4.187 ± 2.199
60	5.671 ± 2.079	3.379 ± 2.184	2.132 ± 0.782	6.068 ± 2.965
90	4.409 ± 2.072	2.198 ± 1.692	1.366 ± 0.642	4.12 ± 2.334
120	3.618 ± 1.956	1.566 ± 1.311	−1.014 ± 0.548	1.11 ± 0.762
150	3.267 ± 1.865	1.31 ± 1.128	−1.295 ± 0.739	0.572 ± 0.389
180	3.282 ± 1.87	1.322 ± 1.136	0.518 ± 0.296	2.396 ± 1.432
210	3.666 ± 1.967	1.603 ± 1.336	1.632 ± 0.875	3.792 ± 2.211
240	4.499 ± 2.079	2.274 ± 1.732	−0.093 ± 0.043	2.738 ± 1.689
270	5.793 ± 2.072	3.506 ± 2.224	−2.616 ± 0.936	1.448 ± 1.289
300	7.189 ± 1.956	5.141 ± 2.605	−0.853 ± 0.232	4.845 ± 2.373

(c) Continued.

	Bounds on NP Parameter	Branching Fraction ($\times 10^{-28}$)		
θ	$\lvert\lambda'^{\star}_{2k2}\lambda'_{2k1}\rvert \times 10^{-9}$	NP	Interference	Combined
330	8.068 ± 1.865	6.35 ± 2.787	3.346 ± 0.773	10.254 ± 3.561
360	8.026 ± 1.87	6.29 ± 2.78	1.979 ± 0.461	8.826 ± 3.241

(d)

	Bounds on NP Parameter	Branching Fraction ($\times 10^{-26}$)		
θ	$\lvert\lambda'^{\star}_{3k2}\lambda'_{3k1}\rvert \times 10^{-9}$	NP	Interference	Combined
0	8.009 ± 1.87	8.097 ± 3.584	−4.48 ± 1.046	4.328 ± 2.539
30	7.071 ± 1.966	6.448 ± 3.328	−1.768 ± 0.491	5.39 ± 2.836
60	5.671 ± 2.076	4.365 ± 2.818	2.734 ± 1.	7.81 ± 3.818
90	4.418 ± 2.069	2.849 ± 2.188	1.761 ± 0.825	5.32 ± 3.012
120	3.631 ± 1.954	2.035 ± 1.698	−1.304 ± 0.701	1.442 ± 0.997
150	3.282 ± 1.865	1.706 ± 1.466	−1.672 ± 0.951	0.744 ± 0.515
180	3.298 ± 1.87	1.72 ± 1.477	0.666 ± 0.378	3.097 ± 1.854
210	3.684 ± 1.966	2.087 ± 1.734	2.106 ± 1.124	4.904 ± 2.858
240	4.515 ± 2.076	2.955 ± 2.244	−0.115 ± 0.053	3.552 ± 2.19
270	5.803 ± 2.069	4.542 ± 2.874	−3.364 ± 1.2	1.889 ± 1.674
300	7.186 ± 1.954	6.638 ± 3.362	−1.102 ± 0.299	6.247 ± 3.063
330	8.054 ± 1.865	8.181 ± 3.596	4.288 ± 0.992	13.18 ± 4.589
360	8.009 ± 1.87	8.097 ± 3.584	2.543 ± 0.594	11.35 ± 4.178

Table 7: Bounds on NP parameters ($\lvert\lambda'_{ijk}\lambda'_{lmn}\rvert, \theta$) derived from $K \longrightarrow \pi\nu_\alpha\overline{\nu}_\alpha$ for $K_L \longrightarrow \nu_\alpha\overline{\nu}_\alpha$. α (Br_{SM}) is (a) unpolarized (4.29×10^{-27}), (b) e (4.48×10^{-33}), (c) μ (3.34×10^{-29}), (d) τ (4.26×10^{-27}).

(a)

	Bounds on NP Parameter	Branching Fraction ($\times 10^{-26}$)		
θ	$\lvert\Sigma_{i=1}^{3}(\lambda'^{\star}_{ik2}\lambda'_{ik1})\rvert \times 10^{-9}$	NP	Interference	Combined
0	3.465 ± 3.209	1.588 ± 1.583	−1.153 ± 1.067	0.858 ± 0.516
30	3.032 ± 2.653	1.156 ± 1.146	−0.451 ± 0.395	1.128 ± 0.75
60	4.229 ±	1.274 ±	1.213 ±	2.91 ± ....
90	2.972 ±	0.629 ±	0.705 ±	1.757 ± ....
120	2.233 ±	0.355 ±	−0.477 ±	0.301 ± ....
150	1.927 ±	0.264 ±	−0.584 ±	0.103 ± ....
180	1.94 ±	0.268 ±	0.233 ±	0.924 ± ....
210	2.278 ±	0.369 ±	0.775 ±	1.567 ± ....
240	3.062 ±	0.667 ±	−0.046 ±	1.044 ± ....
270	4.357 ±	1.352 ±	−1.503 ±	0.272 ± ....
300	3.078 ± 2.721	1.202 ± 1.193	−0.281 ± 0.248	1.344 ± 0.945
330	3.486 ± 3.233	1.61 ± 1.605	1.104 ± 1.024	3.136 ± 2.63
360	3.465 ± 3.209	1.588 ± 1.583	0.655 ± 0.606	2.666 ± 2.19

(b)

	Bounds on NP Parameter	Branching Fraction ($\times 10^{-32}$)		
θ	$\lvert\lambda'^{\star}_{1k2}\lambda'_{1k1}\rvert \times 10^{-9}$	NP	Interference	Combined
0	8.026 ± 1.87	4.98 ± 2.2	−2.784 ± 0.648	2.641 ± 1.552
30	7.083 ± 1.967	3.96 ± 2.04	−1.088 ± 0.3	3.317 ± 1.74
60	5.671 ± 2.079	2.675 ± 1.725	1.698 ± 0.626	4.818 ± 2.351

(b) Continued.

	Bounds on NP Parameter	Branching Fraction ($\times 10^{-32}$)		
θ	$\lvert\lambda'^{\star}_{1k2}\lambda'_{1k1}\rvert \times 10^{-9}$	NP	Interference	Combined
90	4.408 ± 2.072	1.74 ± 1.34	1.085 ± 0.51	3.27 ± 1.85
120	3.618 ± 1.956	1.24 ± 1.04	−0.808 ± 0.439	0.877 ± 0.601
150	3.267 ± 1.865	1.035 ± 0.895	−1.026 ± 0.589	0.454 ± 0.306
180	3.282 ± 1.87	1.05 ± 0.9	0.41 ± 0.235	1.906 ± 1.136
210	3.666 ± 1.967	1.27 ± 1.06	1.297 ± 0.694	3.012 ± 1.754
240	4.498 ± 2.079	1.8 ± 1.37	−0.076 ± 0.034	2.169 ± 1.336
270	5.793 ± 2.072	2.775 ± 1.765	−2.081 ± 0.749	1.139 ± 1.016
300	7.189 ± 1.956	4.07 ± 2.06	−0.674 ± 0.181	3.84 ± 1.879
330	8.068 ± 1.865	5.025 ± 2.205	2.668 ± 0.617	8.138 ± 2.822
360	8.026 ± 1.87	4.98 ± 2.2	1.57 ± 0.366	6.995 ± 2.566

(c)

	Bounds on NP Parameter	Branching Fraction ($\times 10^{-28}$)		
θ	$\lvert\lambda'^{\star}_{2k2}\lambda'_{2k1}\rvert \times 10^{-9}$	NP	Interference	Combined
0	8.026 ± 1.87	3.713 ± 1.641	−2.064 ± 0.481	1.978 ± 1.16
30	7.083 ± 1.967	2.954 ± 1.523	−0.811 ± 0.225	2.472 ± 1.298
60	5.671 ± 2.079	1.995 ± 1.289	1.259 ± 0.461	3.582 ± 1.751
90	4.409 ± 2.072	1.298 ± 1.	0.806 ± 0.378	2.433 ± 1.378
120	3.618 ± 1.956	0.925 ± 0.774	−0.599 ± 0.324	0.655 ± 0.45
150	3.267 ± 1.865	0.774 ± 0.666	−0.764 ± 0.436	0.338 ± 0.23
180	3.282 ± 1.87	0.78 ± 0.671	0.306 ± 0.175	1.414 ± 0.846
210	3.666 ± 1.967	0.946 ± 0.789	0.963 ± 0.517	2.238 ± 1.305
240	4.499 ± 2.079	1.342 ± 1.023	−0.055 ± 0.025	1.616 ± 0.997
270	5.793 ± 2.072	2.07 ± 1.313	−1.544 ± 0.552	0.854 ± 0.76
300	7.189 ± 1.956	3.035 ± 1.538	−0.503 ± 0.136	2.86 ± 1.402
330	8.068 ± 1.865	3.75 ± 1.646	1.976 ± 0.457	6.054 ± 2.102
360	8.026 ± 1.87	3.713 ± 1.641	1.169 ± 0.273	5.211 ± 1.914

(d)

	Bounds on NP Parameter	Branching Fraction ($\times 10^{-26}$)		
θ	$\lvert\lambda'^{\star}_{3k2}\lambda'_{3k1}\rvert \times 10^{-9}$	NP	Interference	Combined
0	8.009 ± 1.87	4.78 ± 2.116	−2.646 ± 0.617	2.555 ± 1.499
30	7.071 ± 1.966	3.806 ± 1.964	−1.044 ± 0.29	3.182 ± 1.674
60	5.671 ± 2.076	2.577 ± 1.663	1.614 ± 0.591	4.611 ± 2.254
90	4.418 ± 2.069	1.682 ± 1.291	1.04 ± 0.487	3.141 ± 1.778
120	3.631 ± 1.954	1.202 ± 1.003	−0.77 ± 0.414	0.851 ± 0.588
150	3.282 ± 1.865	1.007 ± 0.865	−0.988 ± 0.561	0.439 ± 0.304
180	3.298 ± 1.87	1.016 ± 0.871	0.393 ± 0.223	1.828 ± 1.094
210	3.684 ± 1.966	1.233 ± 1.024	1.243 ± 0.664	2.896 ± 1.688
240	4.515 ± 2.076	1.746 ± 1.325	−0.069 ± 0.031	2.096 ± 1.294
270	5.803 ± 2.069	2.682 ± 1.696	−1.986 ± 0.708	1.116 ± 0.988
300	7.186 ± 1.954	3.919 ± 1.985	−0.651 ± 0.177	3.688 ± 1.808
330	8.054 ± 1.865	4.83 ± 2.123	2.531 ± 0.586	7.781 ± 2.709
360	8.009 ± 1.87	4.78 ± 2.116	1.501 ± 0.351	6.701 ± 2.467

Table 8: Bounds on NP parameters ($|\lambda'_{ijk}\lambda'_{lmn}|$,$\theta$) derived from $B \longrightarrow \pi\nu_\alpha\overline{\nu}_\alpha$ for $B_d \longrightarrow \nu_\alpha\overline{\nu}_\alpha$. α (Br_{SM}) is (a) unpolarized (6.35×10^{-25}), (b) e (6.53×10^{-31}), (c) μ (4.87×10^{-27}), (d) τ (6.3×10^{-25})

(a)

	Bounds on NP Parameter		Branching Fraction ($\times10^{-22}$)	
θ	$\left\|\Sigma_{i=1}^{3}\lambda'^{\star}_{ik3}\lambda'_{ik1}\right\| \times 10^{-6}$	NP	Interference	Combined
0	1.0164	3.325	0.269	3.6
30	1.0298	3.413	0.151	3.57
60	1.0506	3.552	−0.23	3.328
90	1.0735	3.709	−0.23	3.485
120	1.0923	3.84	0.168	4.014
150	1.1016	3.905	0.289	4.2
180	1.0987	3.885	−0.08	3.811
210	1.0844	3.784	−0.308	3.482
240	1.0629	3.636	−0.016	3.626
270	1.0402	3.482	0.291	3.779
300	1.0223	3.363	0.104	3.473
330	1.0137	3.307	−0.252	3.061
360	1.0164	3.325	−0.181	3.15

(b)

	Bounds on NP Parameter		Branching Fraction ($\times10^{-27}$)	
θ	$\|\lambda'^{\star}_{1k3}\lambda'_{1k1}\| \times 10^{-6}$	NP	Interference	Combined
0	1.7907	1.06	0.051	1.112
30	1.8043	1.08	0.025	1.106
60	1.8252	1.1	−0.038	1.063
90	1.8481	1.13	−0.04	1.091
120	1.8667	1.15	0.034	1.185
150	1.8759	1.17	0.046	1.217
180	1.873	1.16	−0.012	1.149
210	1.8589	1.14	−0.05	1.091
240	1.8376	1.12	−0.005	1.116
270	1.8148	1.09	0.053	1.144
300	1.7967	1.07	0.018	1.089
330	1.7879	1.06	−0.047	1.014
360	1.7907	1.06	−0.031	1.03

(c)

	Bounds on NP Parameter		Branching Fraction ($\times10^{-23}$)	
θ	$\|\lambda'^{\star}_{2k3}\lambda'_{2k1}\| \times 10^{-6}$	NP	Interference	Combined
0	1.7907	0.792	0.037	0.829
30	1.8043	0.804	0.021	0.825
60	1.8252	0.823	−0.03	0.793
90	1.8481	0.844	−0.03	0.814
120	1.8667	0.861	0.022	0.883
150	1.8759	0.87	0.038	0.908
180	1.873	0.867	−0.01	0.857
210	1.8589	0.854	−0.04	0.814
240	1.8376	0.834	−0.001	0.833
270	1.8148	0.814	0.039	0.853
300	1.7967	0.798	0.014	0.812

(c) Continued.

	Bounds on NP Parameter	Branching Fraction ($\times 10^{-23}$)		
θ	$\lvert\lambda'^{*}_{2k3}\lambda'_{2k1}\rvert \times 10^{-6}$	NP	Interference	Combined
330	1.7879	0.79	−0.034	0.756
360	1.7907	0.792	−0.024	0.768

(d)

	Bounds on NP Parameter	Branching Fraction ($\times 10^{-21}$)		
θ	$\lvert\lambda'^{*}_{3k3}\lambda'_{3k1}\rvert \times 10^{-6}$	NP	Interference	Combined
0	1.7907	1.024	0.047	1.072
30	1.8043	1.04	0.026	1.067
60	1.8252	1.064	−0.04	1.025
90	1.8481	1.091	−0.04	1.052
120	1.8667	1.113	0.028	1.142
150	1.8759	1.124	0.048	1.173
180	1.873	1.12	−0.014	1.107
210	1.8589	1.103	−0.052	1.052
240	1.8376	1.078	−0.003	1.076
270	1.8148	1.052	0.05	1.103
300	1.7967	1.031	0.018	1.05
330	1.7879	1.021	−0.045	0.977
360	1.7907	1.024	−0.032	0.993

TABLE 9: Bounds on NP parameters ($\lvert\lambda'_{ijk}\lambda'_{lmn}\rvert, \theta$) derived from $B \longrightarrow K\nu_\alpha\overline{\nu}_\alpha$ for $B_s \longrightarrow \nu_\alpha\overline{\nu}_\alpha$. α (Br_{SM}) is (a) unpolarized (1.41×10^{-23}), (b) e (1.45×10^{-29}), (c) μ (1.08×10^{-25}), (d) τ (1.4×10^{-23}).

(a)

	Bounds on NP Parameter	Branching Fraction ($\times 10^{-22}$)		
θ	$\lvert\Sigma_{i=1}^{3}(\lambda'^{*}_{ik3}\lambda'_{ik2})\rvert \times 10^{-7}$	NP	Interference	Combined
0	5.9349	1.145	−0.804	0.482
30	5.512	0.988	−0.115	1.014
60	4.4436	0.642	0.574	1.357
90	3.238	0.341	0.197	0.679
120	2.3595	0.181	−0.26	0.062
150	1.9022	0.118	−0.18	0.079
180	1.7667	0.101	0.144	0.386
210	1.9022	0.118	0.228	0.487
240	2.3595	0.181	−0.104	0.218
270	3.238	0.341	−0.432	0.05
300	4.4436	0.642	0.014	0.797
330	5.512	0.988	0.741	1.87
360	5.9349	1.145	0.229	1.515

(b)

	Bounds on NP Parameter	Branching Fraction ($\times 10^{-28}$)		
θ	$\lvert\lambda'^{*}_{1k3}\lambda'_{1k2}\rvert \times 10^{-7}$	NP	Interference	Combined
0	8.7538	2.56	−1.216	1.489
30	8.3927	2.36	−0.183	2.322

(b) Continued.

	Bounds on NP Parameter		Branching Fraction ($\times 10^{-28}$)	
θ	$\lvert \lambda'^{\star}_{1k3}\lambda'_{1k2}\rvert \times 10^{-7}$	NP	Interference	Combined
60	7.4629	1.86	0.996	3.001
90	6.3358	1.34	0.4	1.885
120	5.3788	0.97	−0.612	0.503
150	4.7829	0.77	−0.471	0.444
180	4.5856	0.7	0.387	1.232
210	4.7829	0.77	0.586	1.501
240	5.3788	0.97	−0.246	0.869
270	6.3358	1.34	−0.866	0.619
300	7.4629	1.86	0.028	2.033
330	8.3927	2.36	1.159	3.664
360	8.7538	2.56	0.352	3.057

(c)

	Bounds on NP Parameter		Branching Fraction ($\times 10^{-24}$)	
θ	$\lvert \lambda'^{\star}_{2k3}\lambda'_{2k2}\rvert \times 10^{-7}$	NP	Interference	Combined
0	8.7538	1.913	−0.91	1.111
30	8.3927	1.758	−0.134	1.732
60	7.4629	1.39	0.74	2.238
90	6.3358	1.002	0.296	1.406
120	5.3788	0.722	−0.455	0.375
150	4.7829	0.571	−0.347	0.332
180	4.5856	0.525	0.286	0.919
210	4.7829	0.571	0.44	1.119
240	5.3788	0.722	−0.182	0.648
270	6.3358	1.002	−0.648	0.462
300	7.4629	1.39	0.018	1.516
330	8.3927	1.758	0.867	2.733
360	8.7538	1.913	0.259	2.28

(d)

	Bounds on NP Parameter		Branching Fraction ($\times 10^{-22}$)	
θ	$\lvert \lambda'^{\star}_{3k3}\lambda'_{3k2}\rvert \times 10^{-7}$	NP	Interference	Combined
0	8.7539	2.472	−1.177	1.435
30	8.3927	2.273	−0.174	2.239
60	7.4629	1.797	0.956	2.893
90	6.3357	1.295	0.382	1.817
120	5.3788	0.933	−0.588	0.485
150	4.7829	0.738	−0.45	0.428
180	4.5856	0.678	0.37	1.188
210	4.7829	0.738	0.569	1.447
240	5.3788	0.933	−0.235	0.838
270	6.3357	1.295	−0.838	0.597
300	7.4629	1.797	0.022	1.959
330	8.3927	2.273	1.119	3.532
360	8.7539	2.472	0.335	2.947

References

[1] S. L. Glashow, J. Iliopoulos, and L. Maiani, "Weak interactions with lepton-hadron symmetry," *Physical Review D: Particles, Fields, Gravitation and Cosmology*, vol. 2, no. 7, pp. 1285–1292, 1970.

[2] Y. Fukuda, T. Hayakawa, E. Ichihara, (Super-Kamiokande Collaboration) et al., "Evidence for oscillation of atmospheric neutrinos," *Physical Review Letters*, vol. 81, article 1562, 1998.

[3] G. Mitsuka, K. Abe, Y. Hayato et al., "Study of Non-Standard Neutrino Interactions with Atmospheric Neutrino Data in Super-Kamiokande I and II," *Physical Review D*, vol. 84, article 113008, 2011.

[4] LSND Collaboration, L. B. Auerbach, R. L. Burman, and D. O. Caldwell, "Measurement of electron-neutrino electron elastic scattering," *Physical Review D*, vol. D63, article 112001, 2001.

[5] NuTeV Collaboration, G. P. Zeller, K. S. McFarland, and T. Adams, "A Precise Determination of Electroweak Parameters in Neutrino-Nucleon Scattering," *Physical Review Letters*, vol. 88, article 091802, 2002.

[6] J. A. B. Coelho and (MINOS Collaboration), "Search for effects of exotic models in MINOS Poster," in *Proceedings of the 25th International Conference on Neutrino Physics and Astrophysics (Neutrino 2012)*, Kyoto, Japan, June 2012.

[7] Q. R. Ahmad, (SNO Collaboration) et al., "Measurement of the Rate of νe+d⟶p+p+e−Interactions Produced by 8B Solar Neutrinos at the Sudbury Neutrino Observatory," *Physical Review Letters*, vol. 87, article 071301, 2001.

[8] K. Eguchi, (KamLAND Collaboration) et al., "First Results from KamLAND: Evidence for Reactor Anti-Neutrino Disappearance," *Physics Review Letters*, vol. 90, article 021802, Article ID 021802, 2003.

[9] Z. Isvan and (MINOS Collaboration), "Search for Non-standard Interactions with the MINOS Experiment," https://arxiv.org/abs/1110.1900v1.

[10] F. P. An, J. Z. Bai, A. B. Balantekin et al., "Observation of electron-antineutrino disappearance at Daya Bay," *Physical Review Letters*, vol. 108, article 171803, Article ID 171803, 2012.

[11] Y. Abe, C. Aberle, T. Akiri et al., "Indication for the disappearance of reactor electron antineutrinos in the Double Chooz experiment," *Physical Review Letters*, vol. 108, article 131801, 2012.

[12] Y. Abe, C. Aberle, J. C. dos Anjos, (Double Chooz Collaboration) et al., "Reactor electron antineutrino disappearance in the Double Chooz experiment," *Physical Review D*, vol. 86, article 052008, 2012.

[13] J. K. Ahn, (RENO Collaboration) et al., "Observation of Reactor Electron Antineutrino Disappearance in the RENO Experiment," *Physical Review Letters*, vol. 108, article 191802, 2012.

[14] The Belle Collaboration, H. Tajima et al., "Belle B Physics Results," *International Journal of Modern Physics A*, vol. 2967, no. A17, 2002.

[15] R. Mizuk, R. Chistov et al., "Observation of two resonance-like structures in the π+χc1 mass distribution in exclusive B0⟶K−π+χc1 decays," *Physical Review D*, vol. 78, 072004, 2008.

[16] B. Aubert and (BABAR Collaboration), "Observation of the Semileptonic Decays B⟶D∗τ − $\nu\tau$ and Evidence for B⟶Dτ − $\nu\tau$," *Physical Review Letters*, vol. 100, article 021801, 2008.

[17] A. Paul, I. I. Bigi, and S. Recksiegel, "D0⟶ $\gamma\gamma$ and D0⟶ μ+μ− rates on an unlikely impact of the littlest Higgs model with T parity," *Physical Review D: Particles, Fields, Gravitation and Cosmology*, vol. 83, no. 1, 2011.

[18] Y. Aida, E. Asakawa, G. Cho, and H. Matsuo, "Leptonic decays of Ds and B+ mesons in the supersymmetric standard model with R-parity violating interactions," *Physical Review D: Particles, Fields, Gravitation and Cosmology*, vol. 82, no. 11, 2010.

[19] G. Bhattacharyya, K. Brata Chatterjee, and S. Nandi, "Correlated enhancements in Ds⟶ $\ell\nu$, (g−2) of muon, and lepton flavor violating τ decays with two R-parity violating couplings," *Nuclear Physics B*, vol. 831, article 344, 2010.

[20] B. Bhattacherjee, G. Bhattacharyya, and S. Raychaudhuri, "Can Flavor Physics Hint at Distinctive Signals for R-parity Violation at the LHC?" *Physical Review D*, vol. 84, 075006, 2011.

[21] J. H. Jang, Y. G. Kim, and J. S. Lee, "BXsl+il−j decays with R-parity violation," *Physical Review D*, vol. 58, article 035006, 1998.

[22] Z. Xiao and L. Guo, "B0−B0 mixing and ⟶BXsγ decay in the third type 2HDM: Effects of NLO QCD contributions," *Physical Review D*, vol. 69, article 014002, 2004.

[23] C.-S. Huang, "Neutral Higgs boson contributions to rare leptonic and semi-leptonic B decays in 2HDM and MSSM," *Frontiers of Physics in China*, vol. 2, pp. 212–233, 2007.

[24] J. P. Idarraga, R. Martinez, N. Poveda, and J. A. Rodriguez, "B -> X_s $\gamma$and B+ -> l+ ν in the 2HDM type III," https://arxiv.org/abs/hep-ph/0509072.

[25] R. Ferrandes, "Probing Universal Extra Dimensions through rare decays induced by b⟶s transition," in *Proceedings of the AIP Conference*, vol. 964, article 96, 2007.

[26] Y. Xu, R. Wang, and Y. Yang, "Probe R-parity violating supersymmetry effects in B⟶K(*)ℓ+ℓ− and Bs⟶ ℓ+ℓ− decays," *Physical Review D: Particles, Fields, Gravitation and Cosmology*, vol. 74, no. 11, 2006.

[27] F. De Fazio, *Minneapolis 2006, Continuous advances in QCD*, 2006.

[28] C. S. Kim and R. Wang, " Study of the exclusive ," *Physical Review D: Particles, Fields, Gravitation and Cosmology*, vol. 77, no. 9, 2008.

[29] F. Domingo and U. Ellwanger, "Updated constraints from B physics on the MSSM and the NMSSM," *Journal of High Energy Physics*, vol. 2007, no. 12, pp. 090-090, 2007.

[30] S. Trine, "The MSSM Higgs sector and B-Bbar mixing for large tan(beta)," https://arxiv.org/abs/0710.4955.

[31] Y. Yamada, "b⟶s$\nu\nu$ decay in the MSSM: Implication of b⟶sγ at large tan β," *Physical Review D*, vol. 77, article 014025, 2008.

[32] C. Bobeth, G. Hiller, and G. Piranishvili, "Angular distributions of B ⟶ Kll decays," *Journal of High Energy Physics*, vol. 2007, no. 12, article no. 040, 2007.

[33] I. Ahmed, M. Paracha, and M. Aslam, "Exclusive B⟶K1ℓ+ℓ- decay in model with single universal extra dimension," *The European Physical Journal C*, vol. 54, no. 4, pp. 591–599, 2008.

[34] D. G. Hitlin (Caltech), in *Proceedings of the AIP Conference*, vol. 870, article 398-404, 2006.

[35] A. Palano, Nuclear Physics B - Proceedings Supplements, 156, 105, 2006.

[36] A. Romano, "The K+⟶ π+$\nu\nu$ decay in the NA62 experiment at CERN," https://arxiv.org/abs/1411.6546.

[37] G. D'Ambrosio and A. M. Iyer, "Flavour issues in warped custodial models: B anomalies and rare K decays," https://arxiv.org/abs/1712.08122.

[38] T. K. Komatsubara and Prog. Part, "Experiments with K-Meson Decays," *Progress in Particle and Nuclear Physics*, vol. 67, article 995, 2012.

[39] KOTO Collaboration and K. Shiomi, "$K_0^L \longrightarrow \pi 0 \nu\nu$ at KOTO," in *Proceedings of the 8th International Workshop on the CKM Unitarity Triangle (CKM 2014)*, Vienna, Austria, 2014.

[40] K. F. Chen et al., "B-Physics at CMS with LHC Run-II and Beyond," *Proceedings of Science*, vol. 549, 2015.

[41] Luca. Martini, "The CMS observation of the rare decay B s 0 $\longrightarrow \mu + \mu-$ with the LHC Run I data," *The European Physical Journal Plus*, vol. 130, article 184, 2015.

[42] H. E. Haber and G. L. Kane, "The search for supersymmetry: probing physics beyond the standard model," *Physics Reports*, vol. 117, pp. 75–263, 1985.

[43] R. Haag, J. T. Lopuzanski, and M. F. Sohnius, "All possible generators of supersymmetries of the S-matrix," *Nuclear Physics B*, vol. 88, no. 2, pp. 257–274, 1975.

[44] P. Fayet, Karpacz Winter School (1980) 115 (QC174.45:W5:1980).

[45] S. P. Martin, "A Supersymmetry Primer," *Advanced Series on Directions in High Energy Physics*, vol. 18, pp. 1–98, 1998.

[46] R. Barbier, C. Bérat, and M. Besançon, "*R*-parity-violating supersymmetry," *Physics Reports*, vol. 420, pp. 1–202, 2005.

[47] H. K. Dreiner, M. Kramer, and B. O'Leary, "Bounds on R-parity violating supersymmetric couplings from leptonic and semi-leptonic meson decays," *Physical Review D*, vol. 75, article 114016, 2007.

[48] R. Haag, J. T. Lopuszanski, and M. Sohnius, "All possible generators of supersymmetries of the *S*-matrix," *Nuclear Physics B*, vol. 88, pp. 257–274, 1975.

[49] W. Buchmüller and D. Wyler, "*CP* violation and *R* invariance in supersymmetric models of strong and electroweak interactions," *Physics Letters B*, vol. 121, no. 5, pp. 321–325, 1983.

[50] F. Tahir, M. A. Mughal, and K. Ahmed, "Europhysics Letters 54," pp. 580-585, 2001.

[51] A. Mir, F. Tahir, M. Q. Haseeb, and K. Ahmed, "Implications of *R* parity violating Yukawa couplings in $\Delta S = 1$ semileptonic decays of *K* mesons," *Physical Review D: Particles, Fields, Gravitation and Cosmology*, vol. 76, no. 11, 2007.

[52] A. Mir, F. Tahir, and K. Ahmed, "epton polarization asymmetry in B⟶l+l- decays in R-parity–violating minimal supersymmetric standard model," *Europhysics Letters*, vol. 83, no. 4, 2008.

[53] T. Inami and C. S. Lim, "Effects of superheavy quarks and leptons in low-energy weak processes $K_L \longrightarrow \mu\overline{\mu}$, $K^+ \longrightarrow \pi^+\nu\overline{\nu}$ and $K^0 \longleftrightarrow \overline{K}^0$," *Progress of Theoretical and Experimental Physics*, vol. 65, p. 287, 1981.

[54] N. Cabibbo, "Unitary symmetry and leptonic decays," *Physical Review Letters*, vol. 10, no. 12, pp. 531–533, 1963.

[55] M. Kobayashi and K. Maskawa, "CP Violation in the Renormalizable Theory of Weak Interaction," *Progress of Theoretical Physics*, vol. 49, pp. 652–657, 1973.

[56] D. Rein and L. M. Sehgal, " Long-distance contributions to the decay ," *Physical Review D: Particles, Fields, Gravitation and Cosmology*, vol. 39, no. 11, pp. 3325–3329, 1989.

[57] F. Tahir, M. Anwar Mughal, and K. Ahmed, "New bounds on the products of R-parity breaking couplings from two-body pseudoscalar mesonic decays," *Europhysics Letters*, vol. 54, no. 5, 2001.

[58] K. Lee and P. Yi, "Monopoles and instantons on partially compactified D-branes," *Physical Review D: Particles, Fields, Gravitation and Cosmology*, vol. 56, no. 6, pp. 3711–3717, 1997.

[59] J. Jang, J. K. Kim, and J. S. Lee, " Constraints on the ," *Physical Review D: Particles, Fields, Gravitation and Cosmology*, vol. 55, no. 11, pp. 7296–7299, 1997.

[60] J. Jang, Y. G. Kim, and J. S. Lee, "R-parity violation and semileptonic decays of B-meson," *Physics Letters B*, vol. 408, no. 1-4, pp. 367–372, 1997.

[61] D. Choudhury and P. Roy, "New constraints on lepton nonconserving R-parity violating couplings," *Physics Letters B*, vol. 378, no. 1-4, pp. 153–158, 1996.

[62] A. J. Buras, "Weak Hamiltonian, CP violation and rare decays," https://arxiv.org/abs/hep-ph/9806471.

[63] A. J. Buras, D. Buttazzo, J. Girrbach-Noe, and R. Knegjens, "K+⟶ $\pi+\nu\nu$ and KL⟶ $\pi 0\nu\nu$ in the Standard Model: status and perspectives," *Journal of High Energy Physics*, vol. 33, 2015.

[64] J. Jang, Y. G. Kim, and J. S. Lee, "$BX_s l_i^+ l_j^-$ decays with R-parity violation," *Physical Review D: Particles, Fields, Gravitation and Cosmology*, vol. 58, no. 3, 1998.

[65] W. J. Marciano and Z. Parsa, "Rare kaon decays with "missing energy"," *Physical Review D: Particles, Fields, Gravitation and Cosmology*, vol. 53, no. 1, pp. R1–R5, 1996.

[66] J. L. Rosner, S. Stone, and R. S. Van de, "Leptonic Decays of Charged Pseudoscalar Mesons - 2015," https://arxiv.org/abs/1509.02220.

[67] W. Wang and Z. Xiao, " Semileptonic decays ," *Physical Review D: Particles, Fields, Gravitation and Cosmology*, vol. 86, no. 11, 2012.

[68] C. Patrignani, (Particle Data Group) et al., "Review of Particle Physics," *Chinese Physics C*, vol. 40, no. 10, Article ID 100001, 2016.